UDK 621.791.724:546.82
Original scientific article/Izvirni znanstveni članek

ISSN 1580-2949
MTAEC9, 58(5)549(2024)

DEVELOPING A NUMERICAL MODEL TO OPTIMISE THE LASER-BEAM-WELDING PARAMETERS FOR JOINING TITANIUM TUBES

RAZVOJ NUMERIČNEGA MODELA OPTIMIZACIJE PARAMETROV LASERSKEGA VARJENJA ZA MEDSEBOJNO SPAJANJE CEVI IZ TITANA

Haitham M. Alswat

Department of Mechanical Engineering, College of Engineering, Shaqra University, Dawadmi, Riyadh 11911, Saudi Arabia

Prejem rokopisa – received: 2024-06-19; sprejem za objavo – accepted for publication: 2024-08-16

doi:10.17222/mit.2024.1220

In this work Nd:YAG laser beam welding (LBW), which requires a low heat input, was applied to join grade-2 titanium tubes. The pulse duration and pulse energy were varied according to a two-factor three-level central composite face-centred (CCFC) design to join grade-2 titanium tubes. A numerical model was developed to correlate LBW process parameters and ultimate tensile strength (UTS). Validation of the developed model was done using the analysis of variance. Pulse duration has a more significant impact compared to pulse energy. The highest and lowest values of each process parameter produced a weak UTS, which was less than 338 MPa. The change in the UTS for each process parameter was analysed with metallurgical studies of the joints. Optimised process parameters for improved UTS were identified and reported.

Keywords: laser beam welding, numerical model, titanium tube joints, ultimate tensile strength, optimisation

V članku avtorji opisujejo raziskavo laserskega varjenja (LBW, angl.: laser beam welding) z Nd:YAG laserskim snopom, ki načeloma poteka z manjšim vnosom toplotne energije in so ga uporabili za medsebojno spajanje cevi iz titana kakovosti 2 (Ti-2). Med preizkusi so avtorji analizirali vpliv spreminjanja časa impulzov in količine vnešene energije na tri-nivojsko centralno-čelni način medsebojnega spajanja (CCFC, angl: central composite face-centred design) cevi iz Ti-2. Avtorji so razvili numerični model, ki medsebojno povezuje procesne parametre LBW in končno natezno trdnost (UTS; angl.: ultimate tensile strength) zvarnih spojev. Za ovrednotenje in veljavnost razvitega modela so avtorji uporabili metodo analize variance. Čas trajanja impulzov je mnogo bolj vplival na kakovost zvarov kot količina vnešene toplotne energije. Najvišja in najnižja vrednost obeh izbranih parametrov je rezultirala v najnižjih vrednostih končne natezne trdnosti in sicer manj kot 338 MPa. Spremembo končne natezne trdnosti za vsak izbrani parameter varjenja so analizirali s pomočjo metalurških preiskav na izdelanih zvarnih spojih. V članku poročajo o optimalnih procesnih parametrih, ki dajejo navišjo končno natezno trdnost zvarnih spojev.

Ključne besede: varjenje z laserskim snopom, numerični model, spajanje cevi iz titana, natezna trdnost, optimizacija

1 INTRODUCTION

Titanium alloys are commonly used in aerospace and marine industries due to their high strength and low density. The desirable properties of titanium alloys include excellent resistance to corrosion, high creep strength, high-temperature resistance, high specific strength, etc. Titanium weldment is required in structural and mechanical equipment such as gas turbine blades, rocket engine cases, engine frames, heat exchangers and landing gear of the aircraft and propeller shaft, pressure vessels and fasteners.[1–3] The joining of titanium tubes is widely used in nuclear power plants, marine industry heat exchangers and fuel pipelines for transferring fluids because of its outstanding properties. Titanium alloys have been successfully joined using fusion welding techniques, such as tungsten inert gas welding (TIG) and electron beam welding (EBW). However, defects, poor ductility and a wide heat affected zone caused by TIG welding, and maintaining a high vacuum and a clean environment for EBW are the challenges for the manufacturing industry with respect to joining titanium alloys.[4–5] These challenges can be avoided using friction stir welding (FSW). In FSW, tool manufacturing is another challenge for the joining of titanium alloys.[6] Thus, the advantages of laser beam welding (LBW) appreciably increase the demand in the manufacturing industry. Reduced distortion, a narrow heat-affected zone (HAZ), high-intensity light source, and high scanning speed are the major advantages of LBW for achieving good welds. The complex geometry of a weld is likely to require LBW allowing a reduced production time, high strength, and good microstructural properties.[7] Several studies on joining titanium alloys have confirmed that welding speed, laser power, pulse duration, focal distance, pulse energy, laser frequency, shielding gas, etc., are important process parameters in LBW.[8–15]

Akbari et al.[8] developed an artificial neural network model to analyse the input parameter on the weld bead geometry. Squillace et al.[9] studied different weld bead

*Corresponding author's e-mail:
halswat@su.edu.sa (Haitham M. Alswat)

geometries, fatigue and tensile strength based on different LBW process parameters. Cao et al.[10] studied different kinds of porosity formation of LBW joints for different welding process parameters. Titanium alloys with a thickness of 1.5 mm were successfully joined and the microstructure of the joints was analysed for different welding speeds.[11] Liu et al.[12] reported that laser power has a significant effect on determining the metallurgical properties of LBW joints. The production time and cost are the major challenges in the manufacturing industry, which can be reduced by developing a numerical model to identify and optimise the process parameters for better results. Different methods for predicting and optimising the LBW process parameters are available. Design of experiment (DOE) is one of the techniques used for a better prediction and optimisation.[13,14] The tensile strength of LBW joints is determined based on the process parameters used during welding.

Casalino et al.[15] investigated the joining of a titanium alloy with LBW using the Taguchi technique to develop the statistical model ANOVA for validation by considering the welding speed, laser power and plate thickness as input parameters. Xiansheng et al.[16] varied the pulse shape, pulse frequency, laser power, weld speed, focal length and shielding gas for welding the titanium shell of a neuro-stimulator using Nd:YAG laser welding. They optimised the welding parameters based on the weld bead geometry using the Taguchi matrix method. Prabakaran et al.[13] varied the laser power, welding speed, and focal distance according to the L9 orthogonal array to optimise the process parameters based on the UTS of LB-welded dissimilar steels. Sivagurumanikandan et al.[17] developed a numerical model using an ANN and RSM to predict and optimise the process parameters for a better tensile strength of Nd:YAG LB-welded steel. The study reported that the process parameters including laser power, focal position, pulse frequency and welding speed have a significant effect on selecting the UTS of LBW joints. Shanthos Kumar et al.[18] optimised process parameters using an RSM with a central composite face-centred design (CCFCD) to join dissimilar alloys by combining the pulse duration, pulse energy and welding speed as the input process parameters of an Nd:YAG laser whereas the tensile strength was the output process parameter. Based on ANOVA, they found that the welding speed has the most significant effect on selecting the tensile strength, followed by pulse energy and pulse duration. According to a literature analysis, LBW of a grade-2 titanium tube using a combination of pulse energy and pulse duration, based on CCFCD, is required to meet the demand of the manufacturing industry. Thus, this investigation was made to identify and optimise the optimum process parameters to improve the tensile behaviour of LB-welded grade-2 titanium tubes using a RSM with CCFCD.

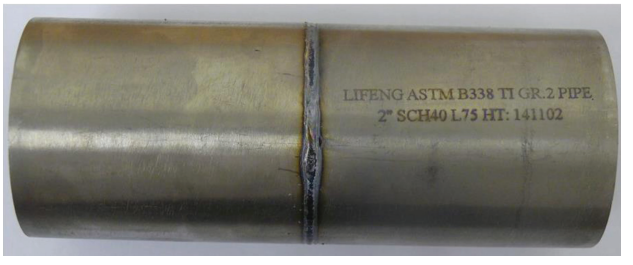

Figure 1: Sample of the LBW grade-2 titanium tube

2 EXPERIMENTAL WORK

LBW has various welding parameters such as laser power, welding speed, focal distance, pulse duration, pulse energy, pulse frequency, pulse shape, shielding gas, etc. Pulse duration and pulse energy are considered as input parameters and their levels are presented in **Table 1**. These ranges of the parameters were identified using a trial experiment. The developed design matrix used to conduct the experimental work is presented in **Table 2**.

Table 1: Process parameters and their levels

Process parameter	Levels		
	–1	0	1
Pulse duration, ms	9	11	13
Pulse energy, J	11	13	15

Table 2: Two-parameter three-level central composite face-centred design

Trail No.	Two-parameter three-level design matrix		Response (ultimate tensile strength, MPa)	
	Pulse duration (T)	Pulse energy (E)	Experimental value, MPa	Predicted value, MPa
1	–1	–1	314.77	314.99
2	1	–1	309.05	309.27
3	–1	1	316.51	316.73
4	1	1	301.31	301.53
5	–1	0	322.39	321.95
6	1	0	311.93	311.49
7	0	–1	333.54	333.10
8	0	1	330.54	330.10
9	0	0	338.79	337.69
10	0	0	336.00	337.69
11	0	0	336.00	337.69
12	0	0	338.00	337.69
13	0	0	338.79	337.69

A grade-2 titanium tube was selected. The chemical composition (in *w*/%) of the commercial grade-2 titanium included 99.69 % Ti and a few other elements – 0.04 % C, 0.10 % Fe, 0.01 % N, 0.09 % O, and 0.007 % H. The outer diameter of the tube was 60 mm, the length of the tube was 75 mm, and the thickness of the tube was approximately 4 mm. Acetone was used to clean the edges of the tube to remove contaminants. Pieces of the tube were clamped using a 3 jaw chuck with a proper alignment. A tack weld was produced before the welding to avoid misalignment. Argon was used as the shielding gas with a flow rate of 15 lpm. An Nd:YAG laser was

Table 3: ANOVA of the developed model

Source	Sum of squares	DOF	Mean square	F-value	P-value	
Model	2055.22	5	411.04	312.88	< 0.0001	
T	164.12	1	164.12	124.92	< 0.0001	
E	13.5	1	13.5	10.28	0.0149	
TE	22.47	1	22.47	17.1	0.0044	significant
T^2	1214.64	1	1214.64	924.56	< 0.0001	
E^2	102.47	1	102.47	78	< 0.0001	
Residual	9.2	7	1.31			
Lack of fit	1.12	3	0.3731	0.1848	0.9016	not significant
Pure error	8.08	4	2.02			
Cor. total	2064.41	12				

used to join the tubes. The upper bead of the weld was protected by keeping the weld shoe inside the tube. A sample of the welded tubes is shown in **Figure 1**.

Tensile specimens as per ASTM E8-04 standard and metallurgical specimens were extracted using a wire EDM machine. Tensile-tested values are presented in **Table 2**. The metallurgical specimens were polished before etching with Kroll's reagent (4 % HNO_3, 2 % HF, 96 % H_2O). After etching, macrographs of the welds were captured using a stereo microscope. To analyse the grain structure of different zones, electron backscattered diffraction (EBSD) was used.

3 RESULTS

3.1 Development of an RSM-based numerical model

A central composite face-centred design (CCFCD) matrix has star points at the centre of each face of factorial space. Thirteen welds were obtained according to the design matrix and the results are presented in Table 2. The relationship between the lower welding process parameters (pulse duration and pulse energy) and the ultimate tensile strength of LBW joints can be presented as a mathematical expression using experimental data. The RSM-based numerical equation for two parameters (pulse duration and pulse energy) with three levels is as follows:

$$Y = F\,(T,E) \tag{1}$$

where:
Y: response (UTS)
T: input parameter 1 (pulse duration)
E: input parameter 2 (pulse energy)

The second-order polynomial equation for the UTS of LBW joints with two parameters is presented by Equation (2) below.

$$UTS = b_0 + b_1T + b_2E + b_{11}T^2 + b_{22}E^2 + b_{12}TE \tag{2}$$

Here, b_0 is the response coefficient for the centre point; b_1 and b_2 are the coefficients of linear terms associated with pulse duration and pulse energy, respectively; b_{11} and b_{22} are the coefficients for the squared terms associated with pulse duration and pulse energy, respectively; b_{12} is the coefficient combining pulse duration and pulse energy. The Design-Expert software version 13 was used to compute all the coefficient values. The regression model developed in a coded form is shown in Equation (3).

$$UTS = 337.69 - 5.23T - 1.5E - 20.97T^2 - \\ - 6.09E^2 - 2.37TE \tag{3}$$

3.2 Adequacy of the developed numerical model

The adequacy of the mathematical model was assessed using ANOVA and the results are presented in **Table 3**. The fitness of statistics of the developed model is presented in **Table 4**.

Table 4: Fitness of statistics of the developed model

Std. dev.	1.15	R^2	0.9955
Mean	325.2	Adjusted R^2	0.9924
C.V. %	0.3525	Predicted R^2	0.9906
	Adequate precision		46.44

The F-values of the developed model (312.88) indicate that the model is significant. Insignificant lack of fit is good for the developed model. The P-values suggest including significant terms to improve the model. The

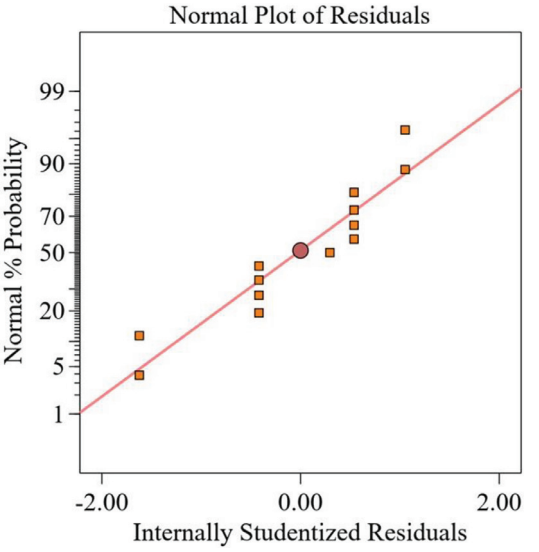

Figure 2: Normal probability of the developed model

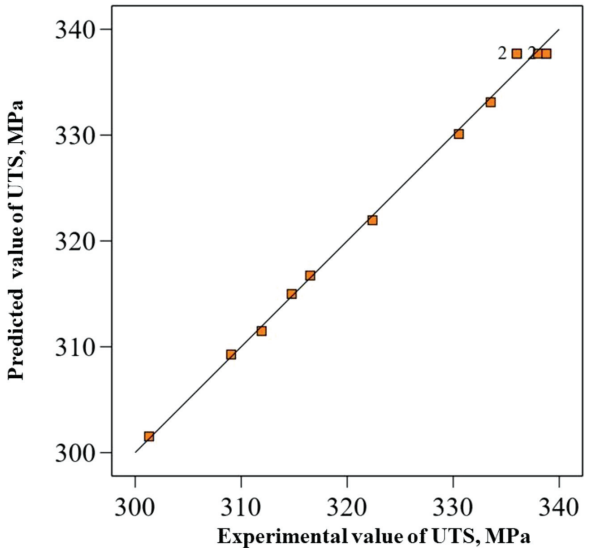

Figure 3: Scatter diagram of the developed model of the LBW of titanium tubes

P-values of linear, quadratic, and interaction terms are significant as they are less than 0.0500. T, E, T^2 and E^2 are significant terms. The coefficient of determination values (R^2) should be 0.6 to 1. In this developed model, the values are more than 0.9. The values of R^2, adjusted R^2 and predicted R^2 agree well. The difference between the predicted R^2 and adjusted R^2 is less than 0.2. The signal-to-noise ratio can be obtained from the adequate precision values.[14] The acceptable range for this ratio is more than 4. The developed model has a ratio of 44.21, which indicates that the developed model is adequate. The normal probability chart for the UTS is shown in **Figure 2**. All the residuals fall in a line, indicating that the error is low for the developed model. A scatter graph was done for experimental and predicted values. All the values are close to the 45-degree line as shown in **Figure 3**. According to the above analysis, the developed model for the LBW of titanium tubes is adequate to use.

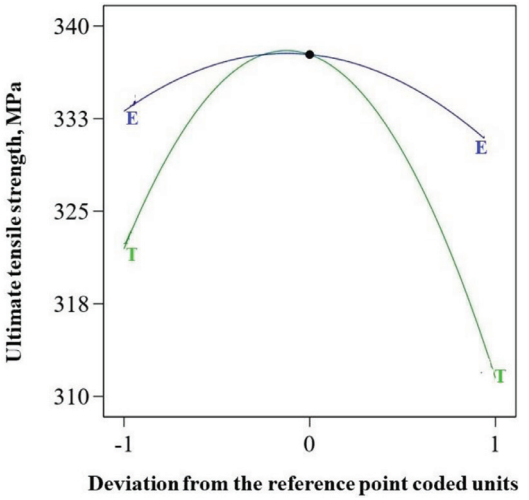

Figure 4: Perturbation diagram of the developed model of the LBW of titanium tubes

A perturbation graph is shown in **Figure 4**, demonstrating the effect of each process parameter on the UTS of the LBW titanium tube. This graph indicates the progress of the responses or output. Although all input parameters deviate from the reference point, the remaining values do not.

4 DISCUSSION

4.1 Effect of the pulse duration and pulse energy on the UTS

The impact of pulse duration and pulse energy on the UTS of titanium tube joints produced by LBW is presented in a response graph, as shown in **Figure 5**.

The response graph illustrates the effects of process parameters and the underlying reasons. An increase in the pulse duration and pulse energy increases the heat input of the LBW, which creates porosity in the joints. Low pulse energy and short pulse duration produce a reduced heat input, which creates undercut defects; this agrees with the work done by Shanthos Kumar et al.[18] High pulse energy and long duration produce a higher heat input, creating porosity in the WZ. Thus, the optimum heat input is required to produce defect-free joints, allowing better mechanical and metallurgical properties than those obtained at higher and lower heat input. The UTS of the titanium tube joints increases with an in-

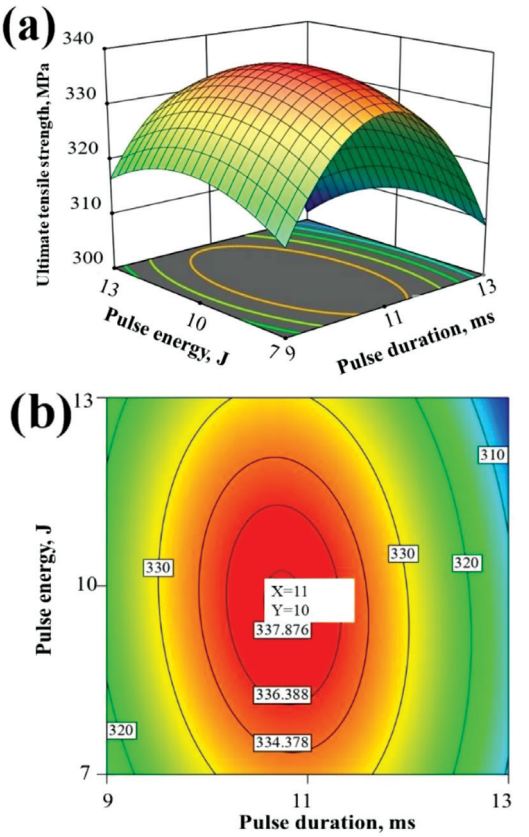

Figure 5: a) Response surface graph of the LBW of titanium tubes; b) contour graph of the LBW of titanium tubes

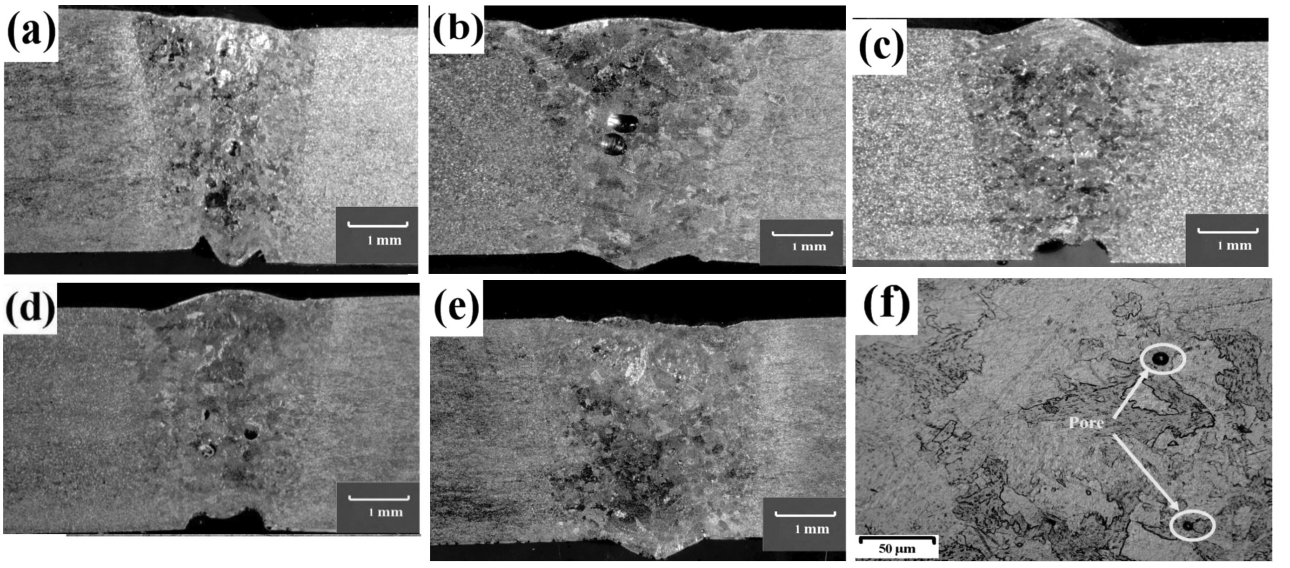

Figure 6: Micrographs of the LBW of titanium tubes: a) pulse duration of 9 ms and pulse energy of 10 J; b) pulse duration of 13 ms and pulse energy of 10 J; c) pulse energy of 7 J and pulse duration of 11 ms; d) pulse energy of 13 J and pulse duration of 11 ms; e) pulse duration of 11 ms and pulse energy of 10 J; f) observed porosity in the WZ

crease in the pulse energy from 7 J to 10 J. Further increment in the pulse energy, from 10 J to 13 J, decreases the UTS of the LBW joints.

It was observed from the microstructure analysis that the lowest UTS occurred due to a low heat input at the lowest pulse energy, resulting in defects at the bottom of the WZ, as shown in **Figure 6a**. The highest pulse energy of 13 J produced an enormous amount of heat at the joints, creating porosity (**Figure 6f**) and causing tensile failure during a tensile-strength test. A similar trend was observed with the pulse duration. Increasing the pulse duration from 9 ms to 11 ms increases the UTS, and from 11 ms to 13 ms, it decreases the UTS. Undercut and porosity are observed at the lowest and highest pulse duration, respectively. Both pulse energy and pulse duration significantly impact the weld bead geometry. The width of the WZ is almost the same from top to bottom at a pulse energy of 10 J and a pulse duration of 11 ms. The WZ is nearly parallel to the joint line at the optimum heat input. It was possible to study the effect of process parameters on the penetration of the joints as part of this work. Grain-size variation was observed in the EBSD images of the LBW of titanium tubes, as shown in **Figure 7**. The BM, HAZ and WZ have different grain sizes. The changes in the microstructure occurred due to the thermal cycle during LBW. The grain-size difference between the WZ and BM is clearly visible. At the same time, the grain-boundary difference between the WZ and HAZ is unclear. Labelling is approximately carried out at the grain border by taking into account the weld root and weld toe position.[7] The HAZ and WZ have coarse grains. Elongated grains are observed in the HAZ, indicating that the formation of a columnar grain structure accrued at the initial stage of solidification.

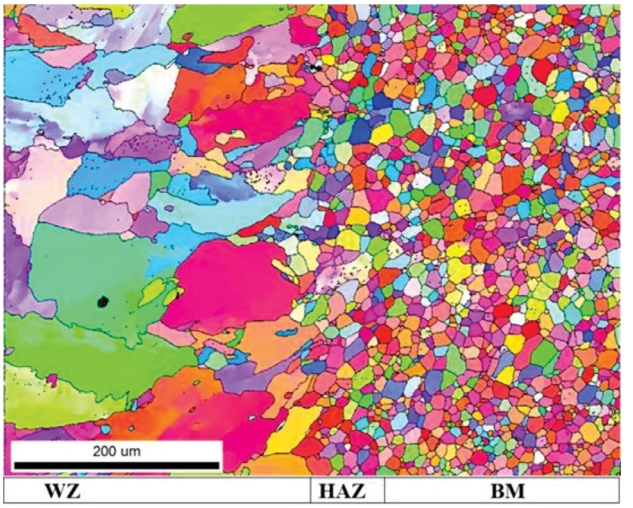

Figure 7: EBSD images of the LBW of titanium tubes comprising WZ, HAZ and BM

The columnar grain structure orients itself along the direction of heat flow during LBW. There are a few definite limits to the width of the HAZ. The uneven and coarse granular grains in the weld zone are caused by the epitaxial growth that occurs during solidification. Li et al.[11] identified a columnar structure in the WZ of pure titanium joints produced by LBW. Similarly, columnar grain structures with irregular coarse grains are observed after the LBW of titanium. Porosity formation is unavoidable with fusion welding methods, including laser welding. The fatigue strength and UTS are determined by the porosity.[7,19]

4.2 Optimisation

RSM is a simple and appropriate technique for designing, analysing, and optimising the process parameter combination for better responses. In RSM, response and

contour plots developed by the numerical model are the indicators used to identify the best process parameters allowing optimised conditions.[13,14] The developed response and contour plots with optimised conditions for the LBW of titanium tubes are presented in **Figure 5**. These plots can predict the output in any range of experimental combinations. The maximum UTS values were taken from the vertex of the response plot. The contour plot was used to predict the optimised values for a better UTS. The vertex point in the contour plot provided the x and y-axis values used to predict the process parameters. The optimised UTS value is 338 MPa, and the corresponding values are a pulse duration of 11 ms and pulse energy of 10 J. In accordance with ANOVA, the process parameters were ranked from the F-ratio. Based on the F-ratio from ANOVA, the pulse duration impacts the UTS more than the pulse energy.

5 CONCLUSION

This study yields the following findings:

- The LBW of titanium tubes was successfully done by considering the pulse duration and pulse energy as the input parameters.
- Using a RSM, a numerical model for optimizing the process parameters of the LBW of titanium tubes was successfully developed.
- Pulse duration and pulse energy are significant process parameters for producing the heat input during LBW, determining the UTS.
- Defects such as undercut and porosity are associated with with low and high heat input, respectively.
- A coarse grain microstructure in the WZ, along with a small HAZ, was identified.
- A pulse duration of 11 ms and a pulse energy of 10 J were the best input parameters for obtaining the highest UTS of 338 MPa.

6 REFERENCES

[1] D. Banerjee, J. C. Williams, Perspectives on Titanium Science and Technology, Acta Materialia, 61 (**2013**), 844–879, doi:10.1016/j.actamat.2012.10.043

[2] W. Zhang, Z. Zhu, C. Y. Cheng, A literature review of titanium metallurgical processes, Hydrometallurgy, 108 (**2011**), 177–188, doi:10.1016/j.hydromet.2011.04.005

[3] Y. Lee, J. Cheon, B. K. Min, C. Kim, Optimization of gas shielding for the vacuum laser beam welding of Ti–6Al–4 V titanium alloy, The International Journal of Advanced Manufacturing Technology, 123 (**2022**), 1297–1305, doi:10.1007/s00170-022-10257-5

[4] A. Karpagaraj, N. Sivashanmugam, K. Sankaranarayanasamy, Some studies on mechanical properties and microstructural characterization of automated TIG welding of thin commercially pure titanium sheets, Materials Science and Engineering A, 640 (**2015**), 180–189, doi:10.1016/j.msea.2015.05.056

[5] M. Wu, R. Xin, Y. Wang, Y. Zhou, K. Wang, Q. Liu, Microstructure, texture and mechanical properties of commercial high-purity thick titanium plates jointed by electron beam welding, Materials Science and Engineering A, 677 (**2016**) 50–57, doi:10.1016/j.msea.2016.09.030

[6] P. D. Edwards, M. Ramulu, Material flow during friction stir welding of Ti-6Al-4V, Journal of Materials Processing Technology, 218 (**2015**), 107–115, doi:10.1016/j.jmatprotec.2014.11.046

[7] R. Palanivel, Effect of laser power on microstructure and mechanical properties of Nd:YAG laser welding of titanium tubes, Journal of Central South University, 30 (**2023**), 1064–1074, doi:10.1007/s11771-023-5292-x

[8] M. Akbari, S. Saedodin, A. Panjehpour, M. Hassani, M. Afrand, M. J. Torkamany, Numerical simulation and designing artificial neural network for estimating melt pool geometry and temperature distribution in laser welding of Ti6Al4V alloy, Optik, 127 (**2016**), 11161–11172, doi:10.1016/j.ijleo.2016.09.042

[9] A. Squillace, U. Prisco, S. Ciliberto, A. Astarita, Effect of welding parameters on morphology and mechanical properties of Ti–6Al–4V laser beam welded butt joints, Journal of Materials Processing Technology, 212 (**2012**), 427–436 doi:10.1016/j.jmatprotec.2011.10.005

[10] X. Cao, A. S. H. Kabir, P. Wanjara, J. Gholipour, A. Birur, J. Cuddy, M. Medraj, Global and Local Mechanical Properties of Autogenously Laser Welded Ti-6Al-4V, Metallurgical and Materials Transactions A, 45 (**2014**), 1258–1272, doi:10.1007/s11661-013-2106-z

[11] C. Li, K. Muneharua, S. Takao, H. Kouji, Fiber laser-GMA hybrid welding of commercially pure titanium, Materials and Design, 30 (2009), 109–114, doi:10.1016/j.matdes.2008.04.043

[12] S. Liu, G. Mi, F. Yan, C. Wang, P. Jiang, Correlation of high-power laser welding parameters with real weld geometry and microstructure, Optics and Laser Technology, 94 (**2017**), 59–67, doi:10.1016/j.optlastec.2017.03.004

[13] M. P. Prabakaran, G. R. Kannan, Optimization of laser welding process parameters in a dissimilar joint of stainless steel AISI316/AISI1018 low carbon steel to attain the maximum level of mechanical properties through PWHT, Optics and Laser Technology, 112 (**2019**), 314–322, doi:10.1016/j.optlastec.2018.11.035

[14] R. Palanivel, S. P. Vigneshwaran, Y. Alqurashi, M. A. Rasheed, Tensile-shear-strength prediction of friction-melt-bonded dissimilar spot joints using RSM, Mater. Tehnol., 57 (**2023**), 57–62, doi:10.17222/mit.2022.689

[15] G. Casalino, F. Curcio, F. Memol Capece Minutolo, Investigation on Ti6Al4V laser welding using statistical and Taguchi approaches, Journal of Materials Processing Technology, 167 (**2005**), 422–428, doi:10.1016/j.jmatprotec.2005.05.031

[16] N. Xiansheng, Z. Zhenggan, W. Xiongwei, L. Luming, The use of Taguchi method to optimize the laser welding of sealing neurostimulator, Optics and Lasers in Engineering, 49 (**2011**), 297–304, doi:10.1016/j.optlaseng.2010.11.005

[17] N. Sivagurumanikandan, S. Saravanan, G. Shanthos Kumar, S. Raju, K. Raghukandan, Prediction and optimization of process parameters to enhance the tensile strength of Nd: YAG laser welded super duplex stainless steel, Optik, 157 (**2018**), 833–840, doi:10.1016/j.ijleo.2017.11.146

[18] G. Shanthos Kumar, K. Raghukandan, S. Saravanan, N. Sivagurumanikandan, Optimization of parameters to attain higher tensile strength in pulsed Nd: YAG laser welded Hastelloy C-276–Monel 400 sheets, Infrared Physics and Technology, 100 (**2019**), 1–10, doi:10.1016/j.infrared.2019.05.002

[19] N. Kashaev, V. Ventzke, V. Fomichev, F. Fomin, S. Riekehr, Effect of Nd: YAG laser beam welding on weld morphology and mechanical properties of Ti–6Al–4V butt joints and T-joints, Optics and Lasers in Engineering, 86 (**2016**), 172–180, doi:10.1016/j.optlaseng.2016.06.004